

## Transmission-based tomography for spin qubits

Amrithesh Sharma<sup>\*</sup> and Ashwin A. Tulapurkar<sup>†</sup>

*Solid State Devices Group, Department of Electrical Engineering, Indian Institute of Technology Bombay, Mumbai, India*

 (Received 12 February 2021; accepted 5 May 2021; published 26 May 2021)

We consider a system of static spin qubits embedded in a one-dimensional spin-coherent channel and develop a scheme to readout the state of one and two qubits separately. We use unpolarized flying qubits for this purpose that scatter off from the static qubits due to localized Heisenberg exchange interaction. Analyzing the transmission coefficient as a function of density matrix elements along with additional unitary gates we reconstruct the state of static qubits.

DOI: [10.1103/PhysRevA.103.052430](https://doi.org/10.1103/PhysRevA.103.052430)

### I. INTRODUCTION

Measurement of the state of qubits is fundamentally crucial for quantum computing [1]. The state, the wave function or the density matrix, of a qubit system is reconstructed from a set of measured observables and is known in literature as state tomography. Since the measurement invokes an interaction of a well-protected quantum system with the observer, the state of the system is inevitably perturbed or in some cases collapsed [2]. The tomography thus involves the simultaneous ensemble measurement of identically prepared states or the repeated measurement of a single state prepared identically for each iteration.

There are a variety of architecture-oriented tomography techniques [3–6]. In this paper we are interested in measuring qubits in spintronic systems, especially those where qubits are housed in localized spins (static qubits) embedded in spin-coherent medium. These types of systems have the potential for scalable fault-tolerant quantum information processing owing to advantages such as long decoherence times, a smaller physical footprint, etc. [7–11]. Manipulation of qubit states in such systems often relies on local magnetic control [12] and or controlled exchange interaction between nearest neighbors [8]. Other approaches found in the literature utilize spin-transfer-torque-like effects for manipulation of single qubits or entangling multiple qubit states using polarized flying qubits [13–21]. Unpolarized flying qubits can also be used for mediating entanglement [22]. From a practical viewpoint local magnetic control is not quite scalable, whereas the latter approaches offer indirect access to remote localized qubits via polarized flying qubits. Polarized flying qubits can be provided by a spin-polarized source through mechanisms such as spin-pumping [23], spin-dependent thermoelectric effects [24], the spin Hall effect [25,26], the spin Nernst effect [27,28], and so on. The control of spin qubits via interaction with flying qubits can be compared to its classical counterpart of manipulating nanomagnets [29–31].

An important aspect of the latter mechanism above is the direct exchange interaction between the spin degrees of freedom of the flying and static qubits. The information in the flying qubit is often not utilized for manipulating the information in static qubits [18,20,21]. The parameters are set such that a single pass (inclusive of multiple scattering inside the channel) of the flying qubits perturbs the combined state of static qubits by a minuscule amount in either reflection or transmission channels. The transmission channel was completely blocked to implement unitary operations in Refs. [18,20,21]. In this work, however, we discuss how we can utilize the information in the flying qubits in the transmission channel to infer the state of static qubits. We specifically analyze the transmission of flying qubits through a system of one qubit and two qubits embedded in a spin-coherent channel. We also assume the contacts at the ends provide flying qubits and perfectly accept the flying qubits without any backscattering into the channel.

The idea of using spin-polarized flying qubits for readout of a single qubit has been discussed in the literature [32,33]. As a major distinction from the previous works, we show that the state of single- and two-qubit systems can be measured by using unpolarized flying electrons. The entanglement between static qubits modulates the transmission coefficient [34] significantly and we show that it can be used to reconstruct not only the subclass of pure states but also the full density matrix.

### II. MODEL

In this section we discuss the one-dimensional problem of scattering of spin-polarized electrons by one or two static impurity spins. The static spins are assumed to be noninteracting with each other, while the incident electron and the static spins are assumed to interact via the Heisenberg exchange interaction. Thus, if the impurity spin is located at  $x = 0$ , the scattering potential is taken as  $\delta(x)J\bar{\sigma}_f \cdot \bar{\sigma}_s$ , where  $\bar{\sigma}_f$  and  $\bar{\sigma}_s$  denote the Pauli spin matrix of the incident electron ( $f$  stands for flying) and the static impurity, respectively, and  $J$  denotes the Heisenberg exchange interaction strength.

*Single impurity with frozen spin.* To begin with, we consider only one static spin and assume the spin of the static impurity to be frozen along the  $\hat{n}$  direction. The transmission coefficient

<sup>\*</sup>amrithesh.iitb@gmail.com; present address: Department of Physics and Astronomy, University of Pittsburgh, Pittsburgh, PA, 15260, USA.

<sup>†</sup>ashwin@ee.iitb.ac.in

( $2 \times 2$  matrix in spin-space) is then given by

$$t = [\mathcal{I}_2 + i\Omega\hat{n} \cdot \sigma_f]^{-1}, \quad (1)$$

where the dimensionless parameter  $\Omega$  is given by  $\Omega = mJ/\hbar^2k$ , where  $m$  and  $k$  denote the mass and the wave vector of the flying electron.  $\mathcal{I}_2$  denotes a  $2 \times 2$  identity matrix. The reflection coefficient is related to the transmission coefficient as  $r = t - \mathcal{I}_2$ . The transmission coefficient can be simplified as  $t = \frac{1}{1+\Omega^2}(\mathcal{I}_2 - i\Omega\hat{n} \cdot \sigma_f)$ . One can see that the factor  $t^\dagger t$  is given by  $t^\dagger t = \frac{1}{1+\Omega^2}\mathcal{I}_2$ . Thus, the transmission probability is independent of the spin direction of the incident electron and is given by  $\frac{1}{1+\Omega^2}$ . However, the incident spin direction is rotated around the  $n$  axis by  $\tan^{-1} \frac{2\Omega}{1-\Omega^2}$  after transmission. Similarly the reflection probability is spin independent, and the reflected spin is rotated around the  $n$  axis by the same angle.

*Two impurities with frozen spins.* We now extend this calculation to two static spin impurities separated by distance  $d$ . We assume that the flying electron interacts via the Heisenberg exchange interaction with both the impurities. We can associate a scattering matrix  $s = [r \ t'; \ t \ r']$  with each impurity, where  $r$  and  $t$  are defined above and  $'$  separates the two rows of the matrix. Further  $r' = r$  and  $t' = t$  here. The combined  $s$  matrix can be calculated from Ref. [35]. The combined transmission coefficient  $t_{\text{comb}}$  under these conditions is given by

$$t_{\text{comb}} = \exp(ikd)t_2[\mathcal{I}_2 - \exp(2ikd)r_1r_2]^{-1}t_1, \quad (2)$$

where the subscripts index the corresponding qubit. Taking the first impurity spin along the  $z$  direction, and the second impurity spin oriented along  $(\theta, \phi)$ , the factor  $t_{\text{comb}}^\dagger t_{\text{comb}}$  turns out to be  $\frac{1}{1+2\Omega^2(1+\cos\theta)}\mathcal{I}_2$ , which is independent of the incident electron spin. Here, we have assumed  $kd \ll 1$  for simplicity. The transmission probability in this case is given by  $P_T = \frac{1}{1+2\Omega^2(1+\cos\theta)}$ . Thus, the transmission probability is again independent of the spin direction of the incident electron. However, the transmission probability depends on the angle between the two static spins. We can consider these two impurities attached to two unpolarized leads, and using the fact that conductance is proportional to the transmission probability, this system shows ‘‘magneto-resistance.’’ The rotation of the spin direction of the incident electron can be found from the transmission and reflection coefficients.

*Single impurity with spin escalated to an operator.* Let us now solve the above two problems assuming the impurity spins to be operators, i.e., treating the impurity spins as qubits. In the case of single static impurity, the transmission coefficient ( $4 \times 4$  matrix) is  $t = [\mathcal{I}_4 + i\Omega\sigma_f \cdot \sigma_s]^{-1}$ . The reflection coefficient is related to  $t$  by  $r = t - \mathcal{I}_4$ .  $t$  is given by

$$t = \frac{1}{1+i\Omega} \begin{bmatrix} 1 & 0 & 0 & 0 \\ 0 & \frac{\Omega+i}{3\Omega+i} & \frac{2\Omega}{3\Omega+i} & 0 \\ 0 & \frac{2\Omega}{3\Omega+i} & \frac{\Omega+i}{3\Omega+i} & 0 \\ 0 & 0 & 0 & 1 \end{bmatrix}. \quad (3)$$

The transmission and reflection probabilities are given by  $P_T = \text{trace}(t^\dagger t \rho)$  and  $P_R = \text{trace}(r^\dagger r \rho)$ , where  $\rho$  is the density matrix of the combined system of an incident electron (flying qubit) and static spin impurity (static spin qubit). Assuming

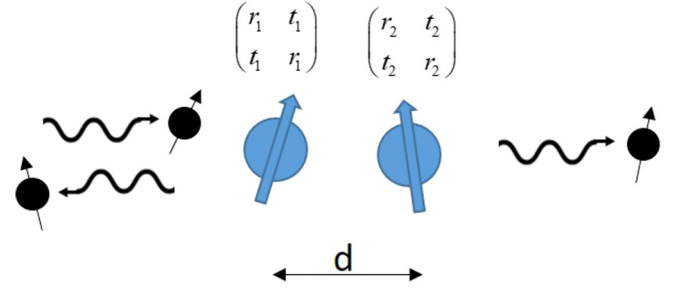


FIG. 1. Scattering of a flying qubit by two static qubits. Individual qubits act as spin-dependent scatterers with reflection and transmission denoted by  $[r]$  and  $[t]$  matrices.

that initially the flying qubit is polarized along the  $z$  direction and the static qubit along the  $(\theta, \phi)$  direction, the transmission probability turns out to be  $P_T = \frac{(7\Omega^2+1)+2\Omega^2\cos(\theta)}{(\Omega^2+1)(9\Omega^2+1)}$ . Note that the transmission probability is independent of the sign of  $\Omega$ . The transmission probability is  $\theta$  dependent, and thus, we get ‘‘magneto-resistance’’ when the impurity spin is treated as an operator. Note magneto-resistance was not seen in the frozen spin case. After the scattering the system is entangled, and the rotation of the spin directions can be found from the transmission and reflection coefficients. The spin of the flying electron develops a spin polarization along the spin direction of the static qubit and there are also changes in the spin polarization in the transverse direction. The same also holds for the static qubit’s spin; i.e., it develops a spin polarization along the spin direction of the flying qubit along with changes in the transverse polarization.

*Two impurities with spins escalated to operators.* We now consider the case of two static qubits. We assume that the static qubits are noninteracting with each other. The flying qubit interacts with each static qubit via Heisenberg exchange interaction. We can associate an  $8 \times 8$  scattering matrix with each static qubit,  $s = [r \ t'; \ t \ r']$ , and combine the two  $s$  matrices to get the combined  $s$  matrix of the system, from which we can find out the transmission and reflection coefficients (see Fig. 1). Knowing the initial density matrix of the combined system of flying and two static qubits, we can find out the transmission probability as  $P_T = \text{trace}(t_{\text{comb}}^\dagger t_{\text{comb}} \rho_i)$ , where  $t_{\text{comb}}$  is the combined transmission matrix and  $\rho_i$  is the initial density matrix. Below we give the expression for transmission probability for the case where the incident flying qubit is unpolarized and the static qubits are described by a density matrix ( $\rho$ ), which was obtained after some algebraic manipulations:

$$P_T = \frac{(1 + 12\Omega^2) + 4\Omega^2(1 + 8\Omega^2)[\rho_{22} + \rho_{33} - 2\text{Re}(\rho_{23})]}{(1 + 16\Omega^2)(1 + 4\Omega^2)}. \quad (4)$$

Note that we have assumed that  $kd \ll 1$  in writing above equation, where  $d$  is the distance between the static qubits. The above equation is valid even for a mixed-state density matrix of static qubits. As the density matrix is positive semidefinite,  $\rho_{22} + \rho_{33} - 2\text{Re}(\rho_{23}) \geq 0$ , which ensures that the transmission probability is non-negative for any value of  $\Omega$ . The factor  $\rho_{22} + \rho_{33} - 2\text{Re}(\rho_{23})$  cannot exceed 2 as

the transmission probability cannot be more than 1. In fact, when this factor is 2, the transmission probability is 1, for any value of  $\Omega$ . As discussed in the Appendix, the above equation can be written in a physically transparent way by noting that  $\frac{1-\langle\sigma_1\cdot\sigma_2\rangle}{2} = \rho_{22} + \rho_{33} - 2\text{Re}(\rho_{23})$ , where  $\sigma_1$  and  $\sigma_2$  are Pauli spin operators of the first and second static qubit, respectively, and  $\langle \rangle$  denotes average value. Further, we can write  $\frac{1-\langle\sigma_1\cdot\sigma_2\rangle}{2} = 2 - \frac{\langle S^2 \rangle}{\hbar^2}$ , where  $S$  is the total spin operator of the two static qubits. Note that the maximum and minimum values of  $\langle S^2/\hbar^2 \rangle$  are 2 and 0, corresponding to the triplet and singlet states, respectively. Thus, the transmission is maximum (equal to 1, for any value of  $\Omega$ ) for the singlet state and minimum for the triplet state. Consider a simple case where the first static qubit is polarized along the  $z$  axis and the second qubit along the  $(\theta, \phi)$  direction. As the qubits are unentangled,  $\langle\sigma_1\cdot\sigma_2\rangle = \langle\sigma_1\rangle\langle\sigma_2\rangle = \cos(\theta)$ . We thus see that the transmission depends on  $\cos(\theta)$ , but the functional form is quite different compared to that of the previous case where the two impurity spins were considered to be frozen. If the static qubit spins are unentangled,  $\langle\sigma_1\cdot\sigma_2\rangle$  ranges from 1 to  $-1$ . In general case, the value of  $\langle\sigma_1\cdot\sigma_2\rangle$  ranges from 1 (triplet state) to  $-3$  (singlet state). Thus, the range of the transmission probability can be significantly increased due to the entanglement.

### III. TOMOGRAPHY SCHEMES

We now examine how tomography of single- and two-qubit system can be performed from the measurement of the transmission probability using unpolarized electrons.

#### A. Tomography of single qubit

Consider a single static impurity qubit with the density matrix to be determined. We assume that multiple copies of the impurity qubit are available. To determine the density matrix, we place an ancilla qubit near the impurity qubit and carry out the transmission measurements using unpolarized flying qubits. If the ancilla qubit is polarized along the  $z$  direction, we can measure the average value  $\langle\sigma_z\rangle$  of the impurity qubit. By changing the polarization of the ancilla qubit to the  $x$  and  $y$  directions, we can measure  $\langle\sigma_x\rangle$  and  $\langle\sigma_y\rangle$  values. From these three average values, the density matrix can be determined as discussed in the Appendix. Instead of rotating the ancilla qubit, one can also rotate the impurity qubit by using single-qubit gates.

#### B. Tomography of a two-qubit system

We now discuss how tomography of the two-qubit system can be carried out by measuring the transmission probability of the incident unpolarized flying qubit. As discussed in the Appendix, to know the density matrix completely we need to find out 15  $a$  coefficients which correspond to the average values of certain operators. We thus need 15 equations relating the  $a$  coefficients. We have seen in the previous section that measurement of the transmission probability depends on  $\langle\sigma_1\cdot\sigma_2\rangle$ ; i.e., it gives us the value of  $(a_{1,1} + a_{2,2} + a_{3,3})$ . We now need two more equations relating  $a_{1,1}$ ,  $a_{2,2}$ , and  $a_{3,3}$  to determine them. We now apply certain gates (unitary

operators,  $U$ ) to the qubit system and measure the transmission probability in the new state ( $\rho_{\text{new}} = U\rho U^\dagger$ ). The gates are chosen to give us the required two equations. Consider applying single qubit  $X$  gate to the second qubit. This corresponds to  $U = \mathcal{I}_2 \otimes \sigma_x$ . One can easily check that  $UM_{1,1}U^\dagger = M_{1,1}$ ,  $UM_{2,2}U^\dagger = -M_{2,2}$ , and  $UM_{3,3}U^\dagger = -M_{3,3}$ , where the various  $M$  matrices are defined in the Appendix. Thus, the values of  $a_{2,2}$  and  $a_{3,3}$  in the new state change sign. Thus, the transmission probability in the new state gives us the value of  $(a_{1,1} - a_{2,2} - a_{3,3})$ . Similarly, measurement of the transmission probability of the state obtained from the original state after application of the  $Y$  gate to the second qubit gives us  $(-a_{1,1} + a_{2,2} - a_{3,3})$ . From these three equations we can obtain  $a_{1,1}$ ,  $a_{2,2}$ , and  $a_{3,3}$ . Instead of applying single-qubit gates to the second qubit, we can as well apply them to the first qubit and will get the same information.

Let us now see how other coefficients can be measured. Consider single-qubit rotation around the  $y$  axis by an amount of  $\pi/2$ . This essentially changes  $z$  into  $x$  and  $x$  into  $-z$ . Thus, taking  $U = \mathcal{I}_2 \otimes R_y(\pi/2)$ , we get  $UM_{1,3}U^\dagger = M_{1,1}$ ,  $UM_{2,2}U^\dagger = M_{2,2}$ , and  $UM_{3,1}U^\dagger = -M_{3,3}$ , i.e.,  $a_{1,1,\text{new}} = a_{1,3}$ ,  $a_{2,2,\text{new}} = a_{2,2}$ , and  $a_{3,3,\text{new}} = -a_{3,1}$ . Thus, measurement of the transmission probability gives the value of  $a_{1,3} - a_{3,1}$ , as the value of  $a_{2,2}$  is known. Now consider the single-qubit gate  $XR_y(\pi/2)$ . Note that the  $X$  gate changes  $y$  into  $-y$  and  $z$  into  $-z$ . Thus, the combined operator  $XR_y(\pi/2)$  changes  $x$  into  $z$  and  $z$  into  $x$  (and  $y$  into  $-y$ ). Thus, by applying  $U = \mathcal{I}_2 \otimes XR_y(\pi/2)$  to the original state and measuring the transmission probability, we get the value of  $a_{1,3} + a_{3,1}$ . From the two equations for  $a_{1,3}$  and  $a_{3,1}$  we can determine them. (Note that  $XR_y(\pi/2)$  is the same as the Hadamard gate.) Using this method, coefficients  $a_{1,2}$  and  $a_{2,1}$  can be determined by the application of  $R_z(\pi/2)$  and  $YR_z(\pi/2)$  single-qubit gates. Similarly, coefficients  $a_{2,3}$  and  $a_{3,2}$  can be determined by the application of  $R_x(\pi/2)$  and  $ZR_x(\pi/2)$  single-qubit gates.

We still need to determine six more coefficients:  $a_{0,i}$  and  $a_{i,0}$  where  $i = 1, 2$ , or  $3$ . These cannot be determined by applying single-qubit gates as index 0 cannot be converted into other nonzero indices by these gates. We need to apply two-qubit gates to get the remaining six  $a$  coefficients. We can choose the square-root SWAP gate as a two-qubit gate. The average  $\langle\sigma_1\cdot\sigma_2\rangle$  is invariant under this operation. However, this gate does change  $M_{0,i}$  and  $M_{i,0}$  matrices, e.g.,  $M_{3,2,\text{new}} = M_{0,1} + M_{1,0}$ . If we apply the single-qubit  $R_x(\pi/2)$  gate on the second qubit after applying the square-root SWAP gate, the resulting transmission probability depends on  $a_{0,1}$  and  $a_{1,0}$ . Applying  $R_z$  on qubit 2, followed by the square-root SWAP gate, followed by  $R_x(\pi/2)$  on qubit 2 gives one more equation for  $a_{0,1}$  and  $a_{1,0}$ . Thus, from these two operations,  $a_{0,1}$  and  $a_{1,0}$  can be determined. In a similar way we can determine  $a_{0,2}$ ,  $a_{2,0}$  and  $a_{0,3}$ ,  $a_{3,0}$ . Note that, in principle, there are many different choices of single- and two-qubit gates. We have selected here some of the ‘‘standard’’ gates naturally implementable in this architecture.

#### 1. Alternative to two-qubit gates

*Using auxiliary static qubits.* It is possible to avoid usage of two-qubit gates in the above scheme. Note that six coefficients,  $a_{i,0}$  and  $a_{0,i}$  with  $i = 1, 2$ , or  $3$ , essentially are

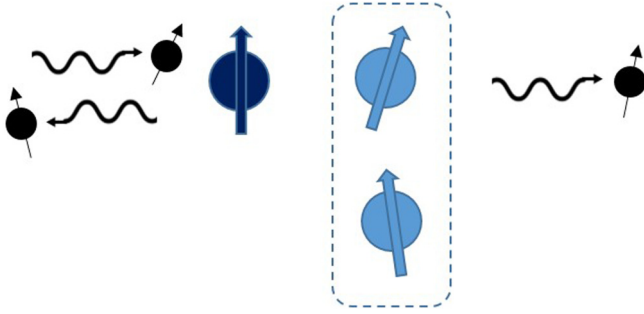


FIG. 2. Measurement of the average spin values of the first qubit. The two static impurity spins are denoted by the color blue. An ancilla qubit is placed near the first static qubit. A flying qubit is passed through the ancilla qubit and the first static qubit.

the average values of  $\sigma_x$ ,  $\sigma_y$ , and  $\sigma_z$  of the first and second qubit, respectively. The average values for the first qubit can be measured as shown in Fig. 2. If the flying qubit interacts only with the first qubit, the transmission probability depends on the average value of  $\sigma$  of the first qubit along the ancilla qubit direction. Thus, by varying the polarization of the ancilla qubit along the  $x$ ,  $y$ , and  $z$  directions we can measure the average values of  $\sigma_x$ ,  $\sigma_y$ , and  $\sigma_z$  of the first qubit. This gives us the coefficients  $a_{1,0}$ ,  $a_{2,0}$ , and  $a_{3,0}$ . Similarly we can carry out the measurements on the second qubit to get  $a_{0,1}$ ,  $a_{0,2}$ , and  $a_{0,3}$ . Note that, in the type of measurements as shown in Fig. 2, what matters is the density matrix traced over the second qubit. It shown in the Appendix that this operation results in a density matrix which depends on the average values of the Pauli operators of the first qubit. As a related comment, it should be noted that any single qubit unitary operation performed on the second qubit does not change the transmission probability through the first qubit, even if the qubits are entangled. It is thus not possible to modulate the transmission via entanglement in such a setting where the other entangled qubit never interacts with the flying qubit. Even if we carry out a projective measurement on the second qubit, the state of the first qubit will also collapse, but the transmission on average still remains the same.

*Using polarized detectors.* Up to now we have considered unpolarized incident flying qubits and looked at the measurement of the transmission probability. If we can also measure the spin polarization of the transmitted flying qubit, we can get additional information. If the flying qubit is transmitted, the density matrix of the system is given by  $t_{\text{comb}}\rho_i t_{\text{comb}}^\dagger / P_T$ . The average value of the flying qubit's Pauli spin operators obtained from the density matrix is given by  $\frac{6\Omega^2}{(1+16\Omega^2)(1+4\Omega^2)} \frac{\langle \sigma_1 + \sigma_2 \rangle}{P_T}$ . Thus, the incident unpolarized flying qubit gets polarized after transmission and the average spin polarization is along the net spin direction of the static qubits. Thus, from these measurements, we can measure  $\langle \sigma_1 \cdot \sigma_2 \rangle$  and  $\langle \sigma_1 + \sigma_2 \rangle$ . In terms of  $a$  coefficients, the measurement of the  $x$ ,  $y$ , and  $z$  components of  $\langle \sigma_1 + \sigma_2 \rangle$  corresponds to measuring  $a_{1,0} + a_{0,1}$ ,  $a_{2,0} + a_{0,2}$ , and  $a_{3,0} + a_{0,3}$ , respectively. If we apply the  $X$  gate to the second qubit, the average value of  $\langle \sigma_{2,y} \rangle$  and  $\langle \sigma_{2,z} \rangle$  changes sign, and we can measure the values of  $a_{2,0} - a_{0,2}$  and  $a_{3,0} + a_{0,3}$ . If we apply the  $Y$  gate to the second qubit, the average value of  $\langle \sigma_{2,x} \rangle$  and  $\langle \sigma_{2,z} \rangle$  changes sign, and

we can measure the values of  $a_{1,0} - a_{0,1}$  and  $a_{3,0} + a_{0,3}$ . Thus, we can measure  $a_{0,123}$  and  $a_{123,0}$  without the need of two qubit gates nor the arrangement shown in Fig. 2.

*Using polarized injectors.* Instead of using an unpolarized incident electron and detecting the polarization of the transmitted electron, we can use a polarized electron as input and then measure the transmission probability. If the incident electron is polarized along the  $z$  direction, the transmission probability is given by  $P_T = \frac{2\Omega^2}{(1+16\Omega^2)(1+4\Omega^2)} (\sigma_{1,z} + \sigma_{2,z})$ , where  $P_T$  is the transmission probability of the unpolarized electron. Thus, measuring the transmission probability with electrons polarized along and opposite to the  $x$ ,  $y$ , and  $z$  directions gives us the values of  $\langle \sigma_1 \cdot \sigma_2 \rangle$  and  $\langle \sigma_1 + \sigma_2 \rangle$ .

### 2. Tomography of a pure two-qubit state

If the two static qubits are in a pure state, we can write the wave function as  $|\psi\rangle = a_1 e^{i\theta_1} |00\rangle + a_2 e^{i\theta_2} [|01\rangle + |10\rangle / \sqrt{2}] + a_3 [|01\rangle - |10\rangle / \sqrt{2}] + a_4 e^{i\theta_3} |11\rangle$ . We have chosen  $\theta_3$  to be 0. There are six unknown parameters due to the normalization condition. We can see that  $\langle \sigma_1 \cdot \sigma_2 \rangle = 1 - 4a_3^2$ . Thus, measurement of the transmission probability of the unpolarized electron gives us the  $a_3$  parameter. As done previously, we can apply various gates to the static qubits and measure the transmission probability. If we measure the transmission probability after applying the  $X$ ,  $Y$ , and  $Z$  gates to the second qubit, we can get the amplitudes of all the four wave-function components, i.e.,  $a_1$ ,  $a_2$ ,  $a_3$ , and  $a_4$ . We can apply  $R_x(\pi/2)$ ,  $R_y(\pi/2)$ , and  $R_z(\pi/2)$  gates to the second qubit and measure the transmission probability. This gives us partial information about the phases; e.g., we get the value of  $\sin(\theta_2)$ , leaving an uncertainty of  $\pi - \theta_2$ . If we measure the transmission probability with polarized qubits, such an uncertainty can be removed.

### C. Discussion on choice of parameters

We have assumed Heisenberg exchange interaction between the flying qubit and each static qubit. If the interaction Hamiltonian is invariant under any unitary operation  $U$ , the transmission coefficients  $t_1$  and  $t_2$  and hence the combined  $s$  matrix are also invariant. This implies that if the initial density matrix is transformed under  $U$ , the transmission probability remains the same. The interaction Hamiltonian here is invariant under the rotation of all spins. The previous results, viz., the transmission probability of unpolarized electrons depends on  $\langle \sigma_1 \cdot \sigma_2 \rangle$  and the transmission probability of spins polarized along  $\hat{n}$  depend on  $\langle \sigma_1 \cdot \sigma_2 \rangle$  and  $\langle (\sigma_1 + \sigma_2) \cdot \hat{n} \rangle$ , are consistent with these symmetry arguments. (It should be also noted that the transmission is invariant under time reversal.) We have assumed the parameter  $kd$  to be small; it can differ from  $2n\pi$  by a small amount, in principle, while combining the  $s$  matrices. In general, the transmission depends on the parameter  $\exp(ikd)$  [see Eq. (2)]. However, this does not change the qualitative nature of the transmission probability; i.e., it still depends on  $\langle \sigma_1 \cdot \sigma_2 \rangle$  and  $\langle (\sigma_1 + \sigma_2) \cdot \hat{n} \rangle$ , but the dependence of various coefficients on the  $\exp(ikd)$  factor is more intricate. As an example, the previous result that transmission is 1 for singlet states no longer holds. Nevertheless the results remain unaltered for  $kd = n\pi$ , which

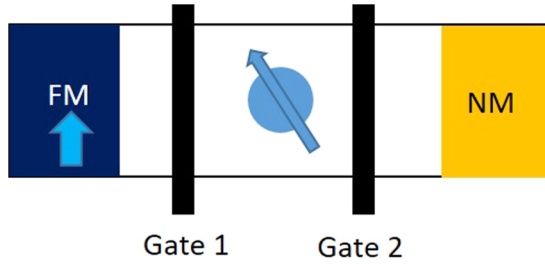


FIG. 3. Heat engine. A static qubit (light blue color) is placed between a ferromagnetic (FM) reservoir and a nonmagnetic (NM) reservoir. By opening gate 1 and closing gate 2, the qubit gets polarized along the magnetization direction of the FM. By opening gate 2 and closing gate 1, the qubit gets depolarized.

is more practical than the  $kd = 0$  limit, and the proposed algorithms for tomography will still work. This argument can be extended to multiple-qubit systems; e.g., in the case of a three-qubit system, the transmission probability would depend on  $\langle \sigma_1 \cdot \sigma_2 + \sigma_2 \cdot \sigma_3 + \sigma_3 \cdot \sigma_1 \rangle$  and  $\langle (\sigma_1 + \sigma_2 + \sigma_3) \cdot \hat{n} \rangle$ . In this way, the present scheme can be extended to tomography of multiple-qubit systems.

We now consider optimizing the values of the parameters ( $kd$  and  $\Omega$ ) for the case of tomography by unpolarized flying qubits. If  $kd = n\pi$ , the transmission coefficient ( $P_T$ ) is one for the singlet state and  $(1 + 12\Omega^2)/(1 + 16\Omega^2)(1 + 4\Omega^2)$  for the triplet state. Thus, a larger value of  $\Omega$  would give a larger variation in the transmission coefficient. In the limit of large  $\Omega$ ,  $P_T$  for the triplet state would be zero. As the  $P_T$  values are at maximum and minimum possible values, the first derivative of  $P_T$  with respect to the parameters  $kd$  and  $\Omega$  is zero, implying that such a choice would be robust against variations in the parameters.

#### IV. AN ALTERNATE APPLICATION

We finally consider another application of the system of flying and static qubits. Consider a static qubit placed between a polarized reservoir and an unpolarized reservoir as shown in Fig. 3. There are two controllable gates between the reservoirs and the static qubit. If we keep gate 2 closed and gate 1 open, the static qubit interacts with the polarized flying qubits incident from the polarized reservoir. The flying qubits finally return to the reservoir as gate 2 acts like a perfect reflector. The flying and static qubits get entangled due to the Heisenberg exchange interaction, and the state of the static qubit is changed when the flying qubit returns to the reservoir, which corresponds to taking a partial trace of the combined density matrix over the flying qubit. This effect has been analyzed in Refs. [18,36] and subsequently in Refs. [20,21]. After sequential interaction with many flying qubits, the static qubit gets polarized along the polarization direction of the reservoir. We now close gate 1 and open gate 2. The static qubit now interacts with unpolarized flying qubits emerging from the second reservoir. After interaction with many flying qubits, the static qubit gets unpolarized. After interaction with the first reservoir, the static qubit's state is a pure state with zero entropy, and after interaction with the second reservoir, the static qubit is in a completely mixed state

with entropy  $k_B \ln(2)$ . Thus, in one cycle a maximum entropy of  $k_B \ln(2)$  can be transferred from the unpolarized reservoir to the polarized reservoir. Thus, the system shown in Fig. 3 can work as a heat engine. We can replace the single qubit by many noninteracting static qubits. Our numerical simulations indicate that it is possible to “magnetize” and “demagnetize” the qubits by connecting them to the ferromagnetic and nonmagnetic reservoirs. The process, however, needs some single-qubit operations on the qubits (which do not change entropy) to completely magnetize and demagnetize the qubits.

#### V. CONCLUSION

In this paper, we have analyzed the transmission of flying qubits from a system of static impurity spins.

The idea of quantum magnetoresistance is discussed whereby the transmission probability and hence the conductance depends on the entangled quantum state of the static qubits. We explicitly obtained the expressions of transmission probability as a function of density matrix components for one or two qubits. The tomography scheme we develop hinges on the fact that the transmission probability through a two-qubit system depends on the expectation value of the scalar product of the spin operators of the two qubits. Measurement of the transmission coefficient after application of appropriate unitary gates is sufficient for inferring the density matrix. For tomography of a single static qubit, we use another ancilla static qubit in a known state. Finally, we discuss another similar scenario containing a single qubit connected to two different types of reservoirs (one polarized and the other unpolarized), each with controlled gates but now utilizing only the reflection channels. Alternating connections to these reservoirs enables the transfer of entropy, which is the tell-tale sign of a minuscule heat engine.

#### ACKNOWLEDGMENTS

We acknowledge the support of the Department of Science and Technology (DST), Government of India, through Project No. SR/NM/NS-1112/2016 and the Science and Engineering Research Board (SERB) through Project No. EMR/2016/007131.

#### APPENDIX

The density matrix for a single qubit can be resolved as

$$\rho = \frac{1}{2}[\mathcal{I}_2 + \langle \sigma_x \rangle \sigma_x + \langle \sigma_y \rangle \sigma_y + \langle \sigma_z \rangle \sigma_z], \quad (\text{A1})$$

where the average of an operator  $O$  is given by  $\langle O \rangle = \text{trace}(\rho O)$ . Thus, the density matrix is uniquely determined if we know  $\langle \sigma_x \rangle$ ,  $\langle \sigma_y \rangle$ , and  $\langle \sigma_z \rangle$ .

For two qubits, the density matrix ( $4 \times 4$ ) can be resolved into 16 matrices obtained from the set  $(\mathcal{I}_2, \sigma_x, \sigma_y, \sigma_z) \otimes (\mathcal{I}_2, \sigma_x, \sigma_y, \sigma_z)$ . We can write

$$\begin{aligned} \rho = & \frac{1}{4}[a_{0,0}(\mathcal{I}_2 \otimes \mathcal{I}_2) + a_{0,1}(\mathcal{I}_2 \otimes \sigma_x) + a_{0,2}(\mathcal{I}_2 \otimes \sigma_y) \\ & + a_{0,3}(\mathcal{I}_2 \otimes \sigma_z) + a_{1,0}(\sigma_x \otimes \mathcal{I}_2) + a_{1,1}(\sigma_x \otimes \sigma_x) \\ & + a_{1,2}(\sigma_x \otimes \sigma_y) + \dots + a_{3,3}(\sigma_z \otimes \sigma_z)]. \quad (\text{A2}) \end{aligned}$$

All the  $a$  coefficients are real and given by  $a_{i,j} = \langle \sigma_i \otimes \sigma_j \rangle$ , where  $\sigma_0 = \mathcal{I}_2$ ,  $\sigma_1 = \sigma_x$ , etc. Note that  $a_{0,0} = 1$  as the trace of the density matrix is 1. We denote the various matrices in the above equation by symbol  $M$ , i.e.,  $M_{i,j} = \sigma_i \otimes \sigma_j$ . To find out the density matrix of the two-qubit system, we need to know these 15 coefficients. Taking the above form of the density matrix, we find that  $\rho_{22} + \rho_{33} - 2\text{Re}(\rho_{23}) = \frac{1}{2}[1 - (a_{1,1} + a_{2,2} + a_{3,3})]$ . Further using,  $a_{1,1} + a_{2,2} + a_{3,3} = \langle \sigma_1 \cdot \sigma_2 \rangle$ , we see that the transmission is determined by  $\langle \sigma_1 \cdot \sigma_2 \rangle$ . Thus, we can write

$$P_T = \frac{(1 + 12\Omega^2) + 2\Omega^2(1 + 8\Omega^2)(1 - \langle \sigma_1 \cdot \sigma_2 \rangle)}{(1 + 16\Omega^2)(1 + 4\Omega^2)}. \quad (\text{A3})$$

If we take the partial trace of the density matrix over the second qubit, we get

$$\rho_1 = \frac{1}{2} \left\{ \mathcal{I}_2 - \begin{bmatrix} a_{3,0} & a_{1,0} - ia_{2,0} \\ a_{1,0} + ia_{2,0} & -a_{3,0} \end{bmatrix} \right\}. \quad (\text{A4})$$

The traced out matrix can be compared to Eq. (A1). It shows that the average values of the Pauli operators of the first qubit in the combined density matrix are the same as average values obtained from the traced out density matrix. Similarly, if we take the partial trace of the density matrix over the first qubit, we get

$$\rho_2 = \frac{1}{2} \left\{ \mathcal{I}_2 - \begin{bmatrix} a_{0,3} & a_{0,1} - ia_{0,2} \\ a_{0,1} + ia_{0,2} & -a_{0,3} \end{bmatrix} \right\} \quad (\text{A5})$$

as the reduced density matrix for the second qubit. The Pauli matrix averages in the reduced density matrix match the corresponding Pauli matrix averages of the second qubit in the combined density matrix. This can be utilized for determining the coefficients appearing in the reduced density matrix without the use of entangling gates as discussed in the main text.

- 
- [1] D. P. DiVincenzo, The physical implementation of quantum computation, *Fortschr. Phys.: Prog. Phys.* **48**, 771 (2000).
- [2] M. A. Nielsen and I. L. Chuang, *Quantum Computation and Quantum Information* (Cambridge University, Cambridge, England, 2010).
- [3] R. Hanson, L. P. Kouwenhoven, J. R. Petta, S. Tarucha, and L. M. K. Vandersypen, Spins in few-electron quantum dots, *Rev. Mod. Phys.* **79**, 1217 (2007).
- [4] C. D. Bruzewicz, J. Chiaverini, R. McConnell, and J. M. Sage, Trapped-ion quantum computing: Progress and challenges, *Appl. Phys. Rev.* **6**, 021314 (2019).
- [5] P. Krantz, M. Kjaergaard, F. Yan, T. P. Orlando, S. Gustavsson, and W. D. Oliver, A quantum engineer's guide to superconducting qubits, *Appl. Phys. Rev.* **6**, 021318 (2019).
- [6] P. Kok, W. J. Munro, K. Nemoto, T. C. Ralph, J. P. Dowling, and G. J. Milburn, Linear optical quantum computing with photonic qubits, *Rev. Mod. Phys.* **79**, 135 (2007).
- [7] S. Bandyopadhyay and M. Cahay, *Introduction to Spintronics* (CRC, Boca Raton, FL, 2015).
- [8] Y. He, S. K. Gorman, D. Keith, L. Kranz, J. G. Keizer, and M. Y. Simmons, A two-qubit gate between phosphorus donor electrons in silicon, *Nature (London)* **571**, 371 (2019).
- [9] E. Ferraro and E. Prati, Is all-electrical silicon quantum computing feasible in the long term? *Phys. Lett. A* **384**, 126352 (2020).
- [10] T. F. Watson, S. G. J. Philips, E. Kawakami, D. R. Ward, P. Scarlino, M. Veldhorst, D. E. Savage, M. G. Lagally, M. Friesen, S. N. Coppersmith, M. A. Eriksson, and L. M. K. Vandersypen, A programmable two-qubit quantum processor in silicon, *Nature (London)* **555**, 633 (2018).
- [11] R. Maurand, X. Jehl, D. Kotekar-Patil, A. Corna, H. Bohuslavskiy, R. Laviéville, L. Hutin, S. Barraud, M. Vinet, M. Sanquer, and S. De Franceschi, A CMOS silicon spin qubit, *Nat. Commun.* **7**, (2016).
- [12] J. J. Pla, K. Y. Tan, J. P. Dehollain, W. H. Lim, J. J. L. Morton, D. N. Jamieson, A. S. Dzurak, and A. Morello, A single-atom electron spin qubit in silicon, *Nature (London)* **489**, 541 (2012).
- [13] K. Yuasa and H. Nakazato, Resonant scattering can enhance the degree of entanglement, *J. Phys. A: Math. Theor.* **40**, 297 (2006).
- [14] A. T. Costa, S. Bose, and Y. Omar, Entanglement of Two Impurities through Electron Scattering, *Phys. Rev. Lett.* **96**, 230501 (2006).
- [15] F. Ciccarello, M. Paternostro, M. Kim, and G. M. Palma, Extraction of Singlet States from Noninteracting High-Dimensional Spins, *Phys. Rev. Lett.* **100**, 150501 (2008).
- [16] K. Yuasa, D. Burgarth, V. Giovannetti, and H. Nakazato, Efficient generation of a maximally entangled state by repeated on- and off-resonant scattering of ancilla qubits, *New J. Phys.* **11**, 123027 (2009).
- [17] F. Ciccarello, D. E. Browne, L. C. Kwek, H. Schomerus, M. Zarcone, and S. Bose, Quasideterministic realization of a universal quantum gate in a single scattering process, *Phys. Rev. A* **85**, 050305(R) (2012).
- [18] B. Sutton and S. Datta, Manipulating quantum information with spin torque, *Sci. Rep.* **5**, 17912 (2016).
- [19] G. Cordourier-Maruri, F. Ciccarello, Y. Omar, M. Zarcone, R. de Coss, and S. Bose, Implementing quantum gates through scattering between a static and a flying qubit, *Phys. Rev. A* **82**, 052313 (2010).
- [20] A. Sharma and A. A. Tulapurkar, Generation of  $n$ -qubit  $W$  states using spin torque, *Phys. Rev. A* **101**, 062330 (2020).
- [21] A. Sharma and A. A. Tulapurkar, Preparation of spin eigenstates including the Dicke states with generalized all-coupled interaction in a spintronic quantum computing architecture, *Quantum Inf. Process.* **20**, 172 (2021).
- [22] F. Ciccarello, M. Paternostro, G. M. Palma, and M. Zarcone, Reducing quantum control for spin-spin entanglement distribution, *New J. Phys.* **11**, 113053 (2009).
- [23] S. Bhuktare, A. S. Shukla, H. Singh, A. Bose, and A. A. Tulapurkar, Direct observation of the reciprocity between spin current and phonon interconversion, *Appl. Phys. Lett.* **114**, 052402 (2019).
- [24] A. Bose, A. K. Shukla, K. Konishi, S. Jain, N. Asam, S. Bhuktare, H. Singh, D. D. Lam, Y. Fujii, S. Miwa *et al.*, Observation of thermally driven field-like spin torque in magnetic tunnel junctions, *Appl. Phys. Lett.* **109**, 032406 (2016).
- [25] A. Bose, S. Dutta, S. Bhuktare, H. Singh, and A. A. Tulapurkar, Sensitive measurement of spin-orbit torque driven

- ferromagnetic resonance detected by planar Hall geometry, *Appl. Phys. Lett.* **111**, 162405 (2017).
- [26] A. Bose, D. D. Lam, S. Bhuktare, S. Dutta, H. Singh, Y. Jibiki, M. Goto, S. Miwa, and A. A. Tulapurkar, Observation of Anomalous Spin Torque Generated by a Ferromagnet, *Phys. Rev. Appl.* **9**, 064026 (2018).
- [27] A. Bose and A. A. Tulapurkar, Recent advances in the spin Nernst effect, *J. Magn. Magn. Mater.* **491**, 165526 (2019).
- [28] A. Bose, S. Bhuktare, H. Singh, S. Dutta, V. G. Achanta, and A. A. Tulapurkar, Direct detection of spin Nernst effect in platinum, *Appl. Phys. Lett.* **112**, 162401 (2018).
- [29] J. C. Slonczewski, Current-driven excitation of magnetic multilayers, *J. Magn. Magn. Mater.* **159**, L1 (1996).
- [30] L. Berger, Emission of spin waves by a magnetic multilayer traversed by a current, *Phys. Rev. B* **54**, 9353 (1996).
- [31] A. S. Shukla, A. Chouhan, R. Pandey, M. Raghupathi, T. Yamamoto, H. Kubota, A. Fukushima, S. Yuasa, T. Nozaki, and A. A. Tulapurkar, Generation of charge current from magnetization oscillation via the inverse of voltage-controlled magnetic anisotropy effect, *Sci. Adv.* **6**, eabc2618 (2020).
- [32] A. De Pasquale, K. Yuasa, and H. Nakazato, State tomography of a qubit through scattering of a probe qubit, *Phys. Rev. A* **80**, 052111 (2009).
- [33] A. De Pasquale, P. Facchi, V. Giovannetti, and K. Yuasa, Entanglement-assisted tomography of a quantum target, *J. Phys. A: Math. Theor.* **45**, 105309 (2012).
- [34] F. Ciccarello, G. M. Palma, M. Zarcone, Y. Omar, and V. R. Vieira, Entanglement controlled single-electron transmittivity, *New J. Phys.* **8**, 214 (2006).
- [35] S. Datta, *Electronic Transport in Mesoscopic Systems* (Cambridge University, Cambridge, England, 1995).
- [36] W. Kim, R. K. Teshima, and F. Marsiglio, How many electrons are needed to flip a local spin? *Europhys. Lett.* **69**, 595 (2005).